An Explicit and Unconditionally Stable FDTD Method for the Analysis of General 3-D Lossy Problems

Md Gaffar and Dan Jiao, *Senior Member, IEEE*

***Abstract*—The root cause of the instability of an explicit finite difference time-domain (FDTD) method is quantitatively identified for the analysis of general lossy problems where both dielectrics and conductors can be lossy and inhomogeneous. Based on the root cause analysis, an efficient algorithm is developed to eradicate the root cause of instability, and subsequently achieve unconditional stability in an explicit FDTD-based simulation of general lossy problems. Numerical experiments have demonstrated the unconditional stability, accuracy, and efficiency of the proposed method.**

***Index Terms*—Explicit methods, finite difference time-domain (FDTD) method, inhomogeneous media, lossy media, time-domain methods, unconditionally stable methods.**

I. Introduction

THE FINITE difference time-domain (FDTD) method has been one of the most popular methods for time-domain analyses [1], [2]. It has gained a wide-spread popularity not only in electromagnetic simulations but also for photonic, thermal, biological, aerodynamic, and many other applications. An explicit FDTD method requires no matrix solution. However, its time step is traditionally restricted by the smallest space step to ensure the stability of a time-domain simulation, as dictated by the Courant–Friedrich–Levy (CFL) condition. When the space step of a given problem can be determined solely from an accuracy point of view, the time step required by the CFL condition has a good correlation with the time step determined by accuracy. However, when the problem involves fine space features relative to working wavelength, which is common in many engineering problems, the time step dictated by the stability condition can be orders of magnitude smaller than the time step required by accuracy. As a result, a tremendous number of time steps need to be simulated to complete one simulation, rendering the overall FDTD simulation computationally expensive, although the computational cost at each time step is trivial.

In contrast to traditional explicit methods that are conditionally stable, in an unconditionally stable method, the choice of time step does not depend on space step, and one can use an infinitely large time step without making a time-domain simulation unstable. In the past decade, a number of implicit unconditionally stable methods have been developed such as the alternating-direction implicit (ADI) method [3], [4], the Crank–Nicolson (CN) method [5], the CN-based split step (SS) scheme [6], the pseudospectral time-domain (PSTD) method [7], the locally one-dimensional (LOD) FDTD [8], [9], the Laguerre FDTD method [10], [11], the associated Hermite (AH) type FDTD [13], a series of fundamental schemes [14], a recent one-step unconditionally stable method [24], and others. In these methods, the time discretization scheme is different from that of an explicit FDTD. It yields an error amplification factor bounded by one irrespective of time step, thus ensuring stability. However, unlike an explicit FDTD method that is free of matrix solution, an implicit FDTD requires solving a matrix. Therefore, it suffers from the issue of computational efficiency when the problem size, and hence matrix size, is large. In [16], a spatial filtering technique has been developed to extend the CFL limit for electromagnetic analysis. The filtering techniques in [15] and [16] have not produced an unconditionally stable method.

Recently, based on the success of an explicit and unconditionally stable time-domain finite-element method [19], an explicit and unconditionally stable FDTD method has been successfully developed in [20] and [21]. This method is stable for an arbitrarily large time step irrespective of space step, and accurate for a time step solely determined by sampling accuracy. Furthermore, it retains the matrix-free property of the original FDTD method, and hence no matrix solution is required. The method does not belong to the class of commonly understood unconditionally stable methods. The essential idea of this method to achieve unconditional stability is to identify the root cause of the instability associated with an explicit marching, and subsequently adapt the underlying numerical system to eradicate the root cause of the instability. As a result, an explicit method can also be made unconditionally stable. On the contrary, the root cause of instability has not been eliminated in existing implicit methods, which is the set of the eigenmodes of the underlying numerical system, whose eigenvalues (characterizing the rate of the space variations of the eigenmodes) are so high that they cannot be accurately simulated by the given time step. This set of unstable eigenmodes exists because of fine discretizations. The fine discretizations cannot be avoided in a structure having fine features relative to working wavelengths. As a consequence, an implicit method

Manuscript received October 28, 2014; revised April 05, 2015; accepted June 08, 2015. Date of publication June 23, 2015; date of current version September 01, 2015. This work was supported in part by the NSF under Grant 0747578 and Grant 1065318 and in part by the DARPA under Grant HR0011-14-1-0057.

The authors are with the School of Electrical and Computer Engineering, Purdue University, West Lafayette, IN 47907 USA (e-mail: djiao@purdue.edu).

Color versions of one or more of the figures in this paper are available online at http://ieeexplore.ieee.org.

Digital Object Identifier 10.1109/TAP.2015.2448751

has to rely on various time integration techniques that have a bounded error amplification factor to control the stability. However, even though the stability is controlled, the presence of these unstable modes, since they cannot be accurately simulated, can still negatively impact the overall solution accuracy and stability in time domain. This will become clear in the sequel.

Despite the success in removing the dependence of the time step on space step, neither [19] nor [20], [21] has addressed the analysis of general lossy problems where dielectrics and conductors are not only inhomogeneous but also lossy. Different from lossless problems where the field solution is governed by a symmetric positive definite generalized eigenvalue problem, whose eigenvalue solutions are real, the field solution of a lossy problem is governed by a quadratic eigenvalue problem whose eigenvalues and eigenvectors are complex-valued. The over-damped eigenmodes, critically damped eigenmodes, and damped oscillations could coexist in the numerical system. Traditionally, the stability analysis of either a purely lossless system or a lossy problem having a uniform conductivity is used to estimate the stability of a lossy problem. However, this approach is not suitable for analyzing the root cause of the instability of an explicit scheme in a general lossy setting, where the lossy materials are inhomogeneous. The root cause of the instability, thus, remains to be thoroughly understood for the analysis of general lossy problems. Furthermore, based on the theory given in [19]–[21], we need to remove certain eigenmodes for the given time step. However, the governing quadratic eigenvalue problem of a lossy problem yields many complex-valued eigenvalues and eigenvectors. Which eigenvalues, and thereby eigenvectors, to remove is unknown for ensuring stability without sacrificing accuracy. In addition, new explicit algorithms need to be devised to achieve unconditional stability for general lossy problems. This paper is written to address these unsolved problems. Numerical examples involving lossy and inhomogeneous dielectrics and conductors, in both closed- and open-region settings, are presented to demonstrate the accuracy, efficiency, and unconditional stability of the proposed explicit method.

The preliminary work of this paper has been reported in our conference papers [22] and [23]. In this paper, we provide a comprehensive and thorough description of the proposed work from theory to methods to numerical experiments. The dispersion error of the proposed method is also theoretically analyzed for not only free-space scenario but also inhomogeneous settings. In addition, we have compared the proposed method with two representative implicit unconditionally stable methods in accuracy, dispersion error, stability, and computational efficiency.

II. Proposed Theory on Making an Explicit FDTD Unconditionally Stable for Analyzing General Lossy Problems

A. Root Cause of Instability

Consider Maxwell's equations governing a general lossy problem having space-dependent conductivity σ, permittivity μ, and permittivity ϵ in a source-free region

$$\nabla \times \mathbf{E} = -\mu \frac{\partial \mathbf{H}}{\partial t}$$
$$\nabla \times \mathbf{H} = \sigma \mathbf{E} + \epsilon \frac{\partial \mathbf{E}}{\partial t}. \tag{1}$$

In the FDTD method, the above continuous equations are essentially discretized into

$$H^{n+\frac{1}{2}} = H^{n-\frac{1}{2}} - \Delta t \mathbf{D}_E E^n \tag{2}$$

$$\left(\mathbf{I} + \frac{\Delta t}{2}\mathbf{D}_\sigma\right) E^{n+1} = \left(\mathbf{I} - \frac{\Delta t}{2}\mathbf{D}_\sigma\right) E^n + \Delta t \mathbf{D}_H H^{n+\frac{1}{2}} \tag{3}$$

where H denotes the vector of unknown magnetic field components, E the vector of unknown electric field components, Δt is the time step, $\mathbf{D}_\sigma$ is a diagonal matrix of element σ/ϵ, $\mathbf{D}_E$ is the sparse matrix representing the discretized $1/\mu\nabla\times$ operator, $\mathbf{D}_H$ represents the discretized $1/\epsilon\nabla\times$ operator, and $\mathbf{I}$ stands for an identity matrix. The superscripts n, $n \pm 1/2$, and $n+1$ denote the time instants. Following (3), the E's value at the nth time step can be written as

$$\left(\mathbf{I} + \frac{1}{2}\Delta t \mathbf{D}_\sigma\right) E^n = \left(\mathbf{I} - \frac{1}{2}\Delta t \mathbf{D}_\sigma\right) E^{n-1} + \Delta t \mathbf{D}_H H^{n-1/2}. \tag{4}$$

Subtracting the above from (3), and substituting (2) into the resultant, we obtain

$$\left(\mathbf{I} + \frac{1}{2}\Delta t \mathbf{D}_\sigma\right) E^{n+1} = 2E^n - \left(\mathbf{I} - \frac{1}{2}\Delta t \mathbf{D}_\sigma\right) E^{n-1} - \Delta t^2 \mathbf{D}_H \mathbf{D}_E E^n \tag{5}$$

which is nothing but a central-difference-based discretization of the following second-order vector wave equation for E

$$\frac{\partial^2 E}{\partial t^2} + \mathbf{D}_\sigma \frac{\partial E}{\partial t} + \mathbf{M} E = 0 \tag{6}$$

where

$$\mathbf{M} = \mathbf{D}_H \mathbf{D}_E. \tag{7}$$

Therefore, from the aforementioned derivation, it can also be seen that the leap-frog based FDTD solution of the first-order Maxwell's equations is essentially a central-difference-based discretization of the second-order wave equation.

The solution of (6), and thereby (5), is governed by the following quadratic eigenvalue problem

$$\left(\lambda^2 + \mathbf{D}_\sigma \lambda + \mathbf{M}\right) V = 0 \tag{8}$$

in which λ denotes the eigenvalue and V is the eigenvector. Since $\mathbf{D}_\sigma$ is positive semidefinite, so is $\mathbf{M}$, the λ of (8) is either real or comes with complex conjugate pairs, and the real part of λ is no greater than zero [17]. The eigenvectors V of (8) are also either real or come with complex conjugate pairs. We can represent E at any time instant rigorously by

$$E(t) = \mathbf{V} y(t) \tag{9}$$

with $\mathbf{V}$ being the eigenvector matrix which represents the column space of the space variation of the field, and $y(t)$ the unknown coefficient vector that is time dependent. In other words, the field solution at any time is a linear superposition of the eigenvectors of the quadratic eigenvalue problem (8).

Now, let us consider an arbitrary eigenvector (eigenmode) of (8) V_i and examine which condition is necessary and sufficient to make this mode be stably simulated in the FDTD-based time marching. For the V_i mode, (5) becomes

$$\left(\mathbf{I}+\frac{1}{2}\Delta t\mathbf{D}_\sigma\right)V_i y_i^{n+1}=2V_i y_i^n-\left(\mathbf{I}-\frac{1}{2}\Delta t\mathbf{D}_\sigma\right)V_i y_i^{n-1}-\Delta t^2\mathbf{D}_H\mathbf{D}_E V_i y_i^n. \tag{10}$$

Front multiplying the above by V_i^H, we have

$$\left(1+\frac{1}{2}\Delta t b_i\right)y_i^{n+1}=2y_i^n-\left(1-\frac{1}{2}\Delta t b_i\right)y_i^{n-1}-\Delta t^2 c_i y_i^n \tag{11}$$

in which b_i and c_i are scalars given by

$$b_i=\frac{V_i^H\mathbf{D}_\sigma V_i}{V_i^H V_i}$$
$$c_i=\frac{V_i^H\mathbf{M}V_i}{V_i^H V_i}. \tag{12}$$

Since both $\mathbf{D}_\sigma$ and $\mathbf{M}$ are positive semidefinites, b_i and c_i are real and no less than zero.

Performing a z-transform of (11), we obtain

$$(z-1)^2+0.5\Delta t b_i(z^2-1)+\Delta t^2 c_i z=0. \tag{13}$$

The roots of the above quadratic equation of z can be readily found as follows:

$$z=\frac{(2-\Delta t^2 c_i)\pm\sqrt{\Delta t^4 c_i^2+\Delta t^2(b_i^2-4c_i)}}{2(1+0.5b_i\Delta t)}. \tag{14}$$

To make (11) stable, $|z|<1$ needs to be satisfied. To obtain the modulus of z, we need to consider all possible scenarios of $b_i^2-4c_i$ as follows.

Since eigenpair (λ_i, V_i) satisfies (8), after front multiplying (8) by V_i^H, we obtain

$$\lambda_i^2+b_i\lambda_i+c_i=0. \tag{15}$$

Thus, the eigenvalue λ_i can be written as

$$\lambda_i=\frac{-b_i\pm\sqrt{b_i^2-4c_i}}{2}. \tag{16}$$

There are three kinds of eigenvalues corresponding to the case of $b_i^2-4c_i>0$, $b_i^2-4c_i=0$, and $b_i^2-4c_i<0$, respectively. The corresponding time-domain solution represents an over-damped, a critically damped, and an under-damped solution, respectively. All of these three cases can exist in the eigenvalue solution of (8). Hence, we must consider all of the three cases when analyzing the roots of z in (14). For each case, we have derived the necessary and sufficient condition that ensures the modulus of (14) bounded by 1, from which we have found that for any given time step Δt, no matter how large it is, the eigenmodes whose eigenvalues satisfy the following condition can be stably simulated by the given time step:

$$\sqrt{c_i}\le\frac{2}{\Delta t}. \tag{17}$$

To understand the meaning of (17) more clearly, it is necessary to reveal the relationship between $\sqrt{c_i}$ and the magnitude of eigenvalues. Consider the under-damped case where $b_i^2-4c_i<0$, from (16), it is evident that

$$\sqrt{c_i}=|\lambda_i| \tag{18}$$

i.e., $\sqrt{c_i}$ is nothing but the magnitude of λ_i. For the critically damped case where $b_i^2-4c_i=0$, we have

$$|\lambda_i|=b_i/2=\sqrt{c_i}. \tag{19}$$

Hence, $\sqrt{c_i}$ is also the magnitude of λ_i. As for the over-damped case of $b_i^2-4c_i>0$, (16) has two distinct values $\lambda_{i1}=\frac{-b_i+\sqrt{b_i^2-4c_i}}{2}$ and $\lambda_{i2}=\frac{-b_i-\sqrt{b_i^2-4c_i}}{2}$, respectively, both of which are negative. It is clear that the following equation holds true:

$$\sqrt{|\lambda_{i1}||\lambda_{i2}|}=\sqrt{c_i}. \tag{20}$$

The above relationship also holds true for the cases shown in (18) and (19). As a result, (17) can be rewritten as

$$\sqrt{|\lambda_{i1}||\lambda_{i2}|}\le\frac{2}{\Delta t}. \tag{21}$$

To understand what happens when (21) is violated and thereby the root cause of instability, it is important to realize that (11) is nothing but a central-difference-based discretization of the following second-order differential equation in time

$$\frac{d^2y}{dt^2}+b_i\frac{dy}{dt}+c_i y=0. \tag{22}$$

Based on the value of $b_i^2-4c_i$, there are three types of solutions of the above equation as follows:

$$y(t)=\begin{cases}Ae^{\lambda_{i1}t}+Be^{\lambda_{i2}t}, & \text{(over-damped)}\\ (A+Bt)e^{\lambda_i t}, & \text{(critically damped)}\\ e^{-b_i/2t}[A\cos(\omega_i t)+B\sin(\omega_i t)], & \text{(under-damped)}\end{cases} \tag{23}$$

where $\omega_i=\frac{\sqrt{4c_i-b_i^2}}{2}$; A and B are arbitrary coefficients.

Now it is ready to analyze the root cause of the instability of an explicit FDTD-based simulation of general lossy problems. To make it clear, we analyze the root cause for each of the three cases one by one.

1) Critically Damped Case: For the critically damped case, $\sqrt{|\lambda_{i1}||\lambda_{i2}|}=|\lambda_i|$. It can be seen from (23) that $|\lambda_i|$ denotes the decay rate of the time-domain solution. As a result, the eigenmodes whose eigenvalues violate (21) have a decay rate faster than that can be accurately sampled by the given time step, and hence they cannot be accurately simulated, thus causing instability. These eigenmodes are the root cause of instability.

2) Under-Damped Case: For the under-damped case, we have $\sqrt{|\lambda_{i1}||\lambda_{i2}|} = |\lambda_i|$. The $|\lambda_i|$ represents the upper bound of the oscillation frequency ω_i. The eigenmodes that violate (21) are also those modes whose oscillation frequencies are too high to be accurately simulated by the given time step Δt, thus causing instability.

3) Over-Damped Case: For the over-damped case, if both λ_{i1} and λ_{i2} satisfy $|\lambda_i| < 2/\Delta t$, (21) would hold true. Therefore, when (21) is violated, at least one of them, specifically λ_{i2}, has a magnitude beyond $2/\Delta t$. Since λ_i for the over-damped case represents the decay rate of the time-domain solution, when $|\lambda_i| > 2/\Delta t$, the corresponding mode decays so fast in time domain that it cannot be accurately captured by the given time step Δt, causing instability.

As a result, we have found that the eigenmodes whose eigenvalues' magnitude exceed $2/\Delta t$ are the root cause of the instability in an explicit FDTD-based simulation of general lossy problems. These eigenmodes exist because of fine space discretization relative to working wavelength. The smaller the space step, the higher the modulus of the eigenvalue of (8). The fine discretization cannot be avoided in structures having small features relative to working wavelength such as integrated circuits operating from zero to microwave frequencies.

B. Making an Explicit FDTD Solution of General Lossy Problems Unconditionally Stable

When the time step is chosen based on accuracy, we have

$$\Delta t \leq \frac{1}{2f_{\max}} \tag{24}$$

where $f_{\max}$ denotes the maximum frequency that exists in the system response based on a prescribed accuracy. The eigenmodes violating (21) have

$$|\lambda_i| > 2/\Delta t. \tag{25}$$

Substituting (24) into (25), we obtain

$$|\lambda_i| > 4f_{\max}. \tag{26}$$

By performing a Fourier transform of (23), it is evident that the unstable eigenmodes satisfying (26) have a frequency beyond the maximum frequency required to be captured by accuracy, and hence they can be removed without sacrificing accuracy. As a result, to make an explicit FDTD-based solution of a general lossy problem unconditionally stable, what we only need to do is to discard the unstable eigenmodes for the given time step. By doing so, we obtain stability without sacrificing accuracy. It is important to note that this statement does not hold true for the spatial Fourier-mode-based expansion like the one used in the Von–Neumann stability analysis, as analyzed in the following section. In addition, if an infinitely large time step is the time step required by accuracy such as simulating a dc problem, we only need to keep the eigenmodes whose eigenvalues are zero, and discard others.

C. Comparison With Von–Neumann Analysis and Accuracy Analysis

In the Von–Neumann stability analysis, the field solution at any time is essentially expanded into the following form:

$$E(\mathbf{r}, t) = \sum_{i=1}^{N} e^{j\mathbf{k}_i \cdot \mathbf{r}} F(\mathbf{k}_i, t) \tag{27}$$

where the space dependence of the field solution is expanded into Fourier modes. Since the time-dependence of each Fourier mode $F(\mathbf{k}_i, t)$ is not analytically known in a general nonfree-space problem, theoretically, it is not feasible to truncate spatial Fourier modes without affecting the accuracy. Take the dc mode whose $\lambda_i = 0$ as an example, this single eigenmode would also have to be represented by many spatial Fourier modes since it has a complicated space dependence in a general inhomogeneous problem. With (27), it is not feasible to use an infinitely large time step to simulate $\lambda_i = 0$ mode stably. In contrast, in the proposed method, the dc mode, whose c_i is zero because a dc mode V has a zero curl and hence satisfying $\mathbf{M}V = 0$, can be simulated by an infinitely large time step without becoming unstable. As can be seen from (17), the time step required for stably simulating $c_i = 0$ modes is infinity.

In the proposed method, by expanding the space dependence of the field solution using the eigenmodes of a governing eigenvalue problem, the time dependence of each mode has an analytical expression as shown in (23). As a result, the modes whose λ_i exceed the maximum frequency required to be captured by accuracy can be removed without affecting the desired accuracy. The aforementioned accuracy analysis is for a source-free problem. For a problem with sources, following the same analysis given in [19], it can be shown that removing eigenmodes that satisfy (26) does not affect the accuracy desired for simulating an $f_{\max}$-based numerical system.

III. Proposed Methods

Based on the aforementioned theoretical analysis, the proposed explicit and unconditionally stable FDTD method has two straightforward steps for the analysis of general lossy problems. The first step is a preprocessing step to find the eigenmodes that can be stably simulated by the given time step no matter how large the time step is. In this step, we develop an efficient algorithm to find the stable eigenmodes instead of solving (8) as it is. This step retains the advantage of the original FDTD in being matrix free. In the second step, we expand the field solution in the solution domain strictly in the space of the stable eigenmodes, and also project the FDTD numerical system onto the space of the stable eigenmodes. As a result, the FDTD-based explicit time marching is absolutely stable for the given time step regardless of the time step size. Next, we first explain the second step, then proceed to elaborate the algorithm of the preprocessing step. In the third part of this section, we also present a diagonal-preserving method to achieve the desired features.

A. Explicit FDTD Marching With Unconditional Stability

We divide the E and H unknowns into two groups. One group is inside the solution domain denoted by subscript S, and the other is outside the solution domain denoted by subscript O, such as unknowns on the boundary or inside an artificial absorber like perfectly matched layer (PML). Subsequently, the sparse matrices $\mathbf{D}_E$ and $\mathbf{D}_H$ can be cast into the following form:

$$\mathbf{D}_E = \begin{bmatrix} \mathbf{D}_{E,SS} & \mathbf{D}_{E,SO} \\ \mathbf{D}_{E,OS} & \mathbf{D}_{E,OO} \end{bmatrix}, \quad \mathbf{D}_H = \begin{bmatrix} \mathbf{D}_{H,SS} & \mathbf{D}_{H,SO} \\ \mathbf{D}_{H,OS} & \mathbf{D}_{H,OO} \end{bmatrix}. \tag{28}$$

With the above, (2) can be rewritten for H_s and H_O as follows:

$$H_S^{n+1/2} = H_S^{n-1/2} - \Delta t \mathbf{D}_{E,SS} E_S^n - \Delta t \mathbf{D}_{E,SO} E_O^n \tag{29}$$

$$H_O^{n+1/2} = H_O^{n-1/2} - \Delta t \mathbf{D}_{E,OO} E_O^n - \Delta t \mathbf{D}_{E,OS} E_S^n. \tag{30}$$

Similarly, (3) can be rewritten as

$$\left(\mathbf{I} + \frac{1}{2}\Delta t \mathbf{D}_\sigma\right) E_S^{n+1} = \left(\mathbf{I} - \frac{1}{2}\Delta t \mathbf{D}_\sigma\right) E_S^n + \Delta t \mathbf{D}_{H,SS} H_S^{n+\frac{1}{2}} + \Delta t \mathbf{D}_{H,SO} H_O^{n+1/2} - \Delta t \mathbf{D}_\epsilon{}^{-1} j^{n+1/2} \tag{31}$$

$$\left(\mathbf{I} + \frac{1}{2}\Delta t \mathbf{D}_\sigma\right) E_O^{n+1} = \left(\mathbf{I} - \frac{1}{2}\Delta t \mathbf{D}_\sigma\right) E_O^n + \Delta t \mathbf{D}_{H,OO} H_O^{n+\frac{1}{2}} + \Delta t \mathbf{D}_{H,OS} H_S^{n+\frac{1}{2}} \tag{32}$$

where $\mathbf{D}_\epsilon$ is a diagonal matrix of element ϵ. The arrangement shown in (29)–(32) is made in view of the fact that the artificial-absorber region such as PML is filled with a single material whose space discretization can be performed solely based on accuracy, while it is the fine feature present in the solution domain that makes the time step smaller than that required by accuracy. Hence, we leave the FDTD solution in the PML region as it is, while performing the time marching in the *solution* domain strictly in the space of the stable modes for the given time step.

For an unconditionally stable simulation of (29) and (31), we expand the unknown fields H_S and E_S strictly in the space of stable eigenmodes for the given time step as follows:

$$\begin{aligned} E_S(t) &= \mathbf{V}_{E,st} y_e(t) \\ H_S(t) &= \mathbf{V}_{H,st} y_h(t) \end{aligned} \tag{33}$$

where y_e and y_h are unknown coefficient vectors which are time dependent, $\mathbf{V}_{E,st}$ is the matrix whose columns are the stable eigenmodes for E, and $\mathbf{V}_{H,st}$ is the same for H. Both $\mathbf{V}_{E,st}$ and $\mathbf{V}_{H,st}$ are independent of time, representing the space variation of the fields only. From (1), it can be seen that the H's space dependence is related to E's dependence by $\mathbf{D}_E$ operator. Therefore, $\mathbf{V}_{H,st}$ can be written as

$$\mathbf{V}_{H,st} = \mathbf{D}_E \mathbf{V}_{E,st}. \tag{34}$$

We also orthogonalize $\mathbf{V}_{E,st}$ to obtain $\tilde{\mathbf{V}}_{E,st}$ so that $\tilde{\mathbf{V}}_{E,st}^H \tilde{\mathbf{V}}_{E,st} = \mathbf{I}$. The same is performed on $\mathbf{V}_{H,st}$ to obtain orthogonalized $\tilde{\mathbf{V}}_{H,st}$. Substituting (33) with orthogonalized stable eigenmodes into (29) and (31), we obtain

$$y_h^{n+1/2} = y_h^{n-1/2} - \Delta t \tilde{\mathbf{V}}_{H,st}^H \mathbf{D}_{E,SS} \tilde{\mathbf{V}}_{E,st} y_e^n - \Delta t \tilde{\mathbf{V}}_{H,st}^H \mathbf{D}_{E,SO} E_O^n \tag{35}$$

$$\begin{aligned} y_e^{n+1} = {} & \tilde{\mathbf{V}}_{E,st}^H \left(\mathbf{I} + 0.5\Delta t \mathbf{D}_\sigma\right)^{-1} \left(\mathbf{I} - 0.5\Delta t \mathbf{D}_\sigma\right) \tilde{\mathbf{V}}_{E,st} y_e^n \\ & + \Delta t \tilde{\mathbf{V}}_{E,st}^H \left(\mathbf{I} + 0.5\Delta t \mathbf{D}_\sigma\right)^{-1} \mathbf{D}_{H,SS} \tilde{\mathbf{V}}_{H,st} y_h^{n+1/2} \\ & + \Delta t \tilde{\mathbf{V}}_{E,st}^H \left(\mathbf{I} + 0.5\Delta t \mathbf{D}_\sigma\right)^{-1} \mathbf{D}_{H,SO} H_O^{n+1/2} \\ & + \Delta t \tilde{\mathbf{V}}_{E,st}^H \left(\mathbf{I} - 0.5\Delta t \mathbf{D}_\sigma\right)^{-1} \mathbf{D}_\epsilon{}^{-1} j^{n+1/2}. \end{aligned} \tag{36}$$

After the unknown coefficient vectors y_e and y_h are found from (35) and (36), the entire field solution can be recovered at any point of interest from (33).

B. Preprocessing for Finding Stable Eigenmodes for the Given Time Step

In the proposed algorithm for finding stable eigenmodes, we start the conventional FDTD simulation of (29)–(32), which is only done for a small time window [when to stop is adaptively controlled by the following (42) and (43)]. At selected time instants such as every pth step ($p \geq 1$ and it is usually chosen as the ratio of the time step determined by sampling accuracy and the time step dictated by stability), we add E field solution E_S in matrix $\mathbf{F}_E$ (initialized to be zero) as one column vector, and also orthogonalize $\mathbf{F}_E$. The column dimension of the orthogonalized $\mathbf{F}_E$ is denoted by k' and its row dimension is denoted by N_e. With $\mathbf{F}_E$, we transform the original large-scale eigenvalue problem (8) to a reduced eigenvalue problem as follows:

$$(\lambda^2 + \lambda \mathbf{D}_{\sigma,r} + \mathbf{M}_r) V_r = 0 \tag{37}$$

in which both $\mathbf{D}_{\sigma,r}$ and $\mathbf{M}_r$ are small matrices of size k', which are given by

$$\begin{aligned} \mathbf{D}_{\sigma,r} &= \mathbf{F}_E^T \mathbf{D}_\sigma \mathbf{F}_E \\ \mathbf{M}_r &= \mathbf{F}_E^T \mathbf{M} \mathbf{F}_E. \end{aligned} \tag{38}$$

The small quadratic eigenvalue problem (37) can be rigorously transformed to a standard eigenvalue problem

$$\begin{bmatrix} \mathbf{0}_{k' \times k'} & \mathbf{I}_{k' \times k'} \\ -\underbrace{\mathbf{M}_r}_{k' \times k'} & -\underbrace{\mathbf{D}_{\sigma,r}}_{k' \times k'} \end{bmatrix} \begin{Bmatrix} V_r \\ \lambda V_r \end{Bmatrix} = \lambda \begin{Bmatrix} V_r \\ \lambda V_r \end{Bmatrix} \tag{39}$$

which can be solved with negligible cost due to its small size.

When progressively adding a solution vector into $\mathbf{F}_E$ in the above process, repeating eigenvalues will appear from the eigenvalue solution of (39). These repeating eigenvalues, when the weights of their eigenvectors become dominant in the field solution, can be identified as the physically important eigenvalues of the original system as analyzed in [19]. To determine the weights, denote the upper half (k' rows) of the eigenmodes of (39) corresponding to the repeating eigenvalues by $\mathbf{V}_{r,l}$, and those of the rest eigenmodes by $\mathbf{V}_{r,h}$. As the matrix in (39)

is not symmetric positive semidefinite, $\mathbf{V}_{r,l}$ and $\mathbf{V}_{r,h}$ are not orthogonal by themselves. To find their weights in the field solution, we cannot use the same procedure as that in [21] developed for the lossless problems. Therefore, we first orthogonalize $\mathbf{V}_{r,l}$ to obtain $\tilde{\mathbf{V}}_{r,l}$, and then exclude the projection of $\mathbf{V}_{r,h}$ onto $\mathbf{V}_{r,l}$ by computing $\hat{\mathbf{V}}_{r,h} = \mathbf{V}_{r,h} - \tilde{\mathbf{V}}_{r,l}\tilde{\mathbf{V}}_{r,l}^H\mathbf{V}_{r,h}$, which is then orthogonalized to a new $\tilde{\mathbf{V}}_{r,h}$. The weights of the repeating eigenmodes and the nonrepeating ones, y_{el} and y_{eh}, can then be determined from

$$[y_{el} \quad y_{eh}]^T = \tilde{\mathbf{V}}_r^H \mathbf{F}_E^H E_S \tag{40}$$

where

$$\tilde{\mathbf{V}}_r = \left[\tilde{\mathbf{V}}_{r,l} \quad \tilde{\mathbf{V}}_{r,h}\right]. \tag{41}$$

The dominance of the repeating eigenmodes $\mathbf{V}_{r,l}$ can be assessed by the ratio of their weights to the weights of the nonrepeating ones as the following:

$$\left|y_{eh}^H y_{eh}\right| / \left|y_{el}^H y_{el}\right| \leq \epsilon_1. \tag{42}$$

The preprocessing step is terminated when the above, as well as the following, is satisfied:

$$\left|\lambda_{i,l}^{j+1} - \lambda_{i,l}^{j}\right| / \left|\lambda_{i,l}^{j}\right| \leq \epsilon_2 \tag{43}$$

in which $\lambda_{i,l}^{j}$ is the ith nonzero repeating eigenvalue observed at the jth step.

When the preprocessing step is terminated, a complete and accurate set of the stable eigenmodes has been identified. Among the repeating eigenmodes observed from (39) step after step, we simply select those whose eigenvalues satisfy (17) to form $\mathbf{V}_{E,st}$ in (33). As a result, we obtain

$$\mathbf{V}_{E,st} = \mathbf{F}_E \mathbf{V}_{r,st} \tag{44}$$

where $\mathbf{V}_{r,st}$ are the repeating eigenmodes identified from the small generalized eigenvalue problem (39) whose eigenvalues satisfy (17).

C. Diagonal-Preserving Formulation

The updating equations shown in (35) and (36) involve the orthogonalization of $\mathbf{V}_{E,st}$, $\mathbf{V}_{H,st}$, and a few matrix–matrix multiplications in the right-hand side. These computations do not depend on time, and hence can be prepared in advance and used for all time steps. The computational complexity of the orthogonalization as well as one matrix–matrix product involved in (35) and (36) is $O(k^2N)$, where k is the number of stable eigenmodes, which is much smaller than the number of E or H unknowns N as analyzed in [21]. In addition, the matrices in (35) and (36) associated with inverses are diagonal matrices, thus the inversion cost is negligible. Despite the aforementioned facts, the computational efficiency of (35) and (36) is still not desirable when k is large. In this section, we present a diagonal-preserving formulation to facilitate the analysis of problems with a large k.

Basically, in lossless problems, the eigenmodes are orthogonal by themselves. They also diagonalize the underlying system matrix. As a result, the resultant time-marching equation is a fully decoupled *diagonal* system of equations when the FDTD numerical system is projected onto the space of stable eigenmodes. Unlike lossless problems, the eigenmodes in a general lossy problem are not orthogonal by themselves; they do not diagonalize the underlying system matrix either. These are the sources of the additional computational cost incurred in (35) and (36) as compared to the updating equations of lossless problems given in [20] and [21].

To overcome the aforementioned problem, we first rewrite (6) as a first-order system as follows:

$$\frac{\partial}{\partial t}\begin{Bmatrix} E \\ \frac{\partial E}{\partial t} \end{Bmatrix} - \begin{bmatrix} \mathbf{0} & \mathbf{I} \\ -\mathbf{M} & -\mathbf{D}_\sigma \end{bmatrix}\begin{Bmatrix} E \\ \frac{\partial E}{\partial t} \end{Bmatrix} = \begin{Bmatrix} 0 \\ f' \end{Bmatrix} \tag{45}$$

which can further be compactly written as

$$\frac{\partial U}{\partial t} - \mathbf{M}_A U = f \tag{46}$$

where

$$\mathbf{M}_A = \begin{bmatrix} \mathbf{0} & \mathbf{I} \\ -\mathbf{M} & -\mathbf{D}_\sigma \end{bmatrix} \tag{47}$$

and

$$U = \begin{Bmatrix} E \\ \frac{\partial E}{\partial t} \end{Bmatrix}. \tag{48}$$

Meanwhile, we can cast (8) into the following generalized eigenvalue problem:

$$\begin{bmatrix} \mathbf{0} & \mathbf{I} \\ -\mathbf{M} & -\mathbf{D}_\sigma \end{bmatrix}\begin{Bmatrix} V \\ \lambda V \end{Bmatrix} = \lambda \begin{Bmatrix} V \\ \lambda V \end{Bmatrix} \tag{49}$$

which can be rewritten in short as

$$\mathbf{M}_A V_A = \lambda V_A. \tag{50}$$

From (49), it can be seen that the upper half of the eigenvector of $\mathbf{M}_A$, V, is the eigenvector of the original (8). If we expand U in (46) by $\mathbf{V}_{A,st}$, the *stable* subset of $\mathbf{V}_A$ satisfying (17), and front multiply (46) by $\mathbf{V}_{A,st}^H$. Utilizing the property of $\mathbf{M}_A\mathbf{V}_{A,st} = \mathbf{V}_{A,st}\mathbf{\Lambda}_{st}$, where $\mathbf{\Lambda}_{st}$ is the diagonal matrix of stable eigenvalues, we can obtain

$$\frac{dy}{dt} - \mathbf{\Lambda}_{st} y = (\mathbf{V}_{A,st}^H \mathbf{V}_{A,st})^{-1}\mathbf{V}_{A,st}^H f \tag{51}$$

which is a diagonal system of equation. Therefore, the diagonal property is preserved in the projected space of stable modes. Furthermore, the computation involved in the right hand side can be done once for all time steps. More important, the overall cost of (51) is less than that of (35) and (36). If there are many stable eigenmodes, as given in [21], we can divide the frequency band of interest into multiple smaller bands. We then find the stable eigenmodes in each small band, the number of which is not large so that the product $\mathbf{V}_{A,st}^H\mathbf{V}_{A,st}$ of $O(k^2N)$

computational cost can be efficiently computed, and the resultant $k \times k$ matrix can be readily inverted. The union of the sable eigenmodes found in each small band forms the stable eigenmodes in the entire frequency band of interest.

To find $\mathbf{V}_{A,st}$ efficiently without solving (50), similar to the preprocessing algorithm described in the previous section, we first obtain a set of time-domain solutions. From these solutions and the system matrix, we determine the stable eigenmodes. To be specific, we perform the time marching of (45) in a leap-frog way, obtaining

$$\left(\mathbf{I}+\frac{\Delta t}{2}\mathbf{D}_\sigma\right)W^{n+1}=\left(\mathbf{I}-\frac{\Delta t}{2}\mathbf{D}_\sigma\right)W^n - \Delta t\mathbf{M}E^{n+\frac{1}{2}}-\Delta t f' \tag{52}$$

$$E^{n+\frac{1}{2}+1}=E^{n+\frac{1}{2}}+\Delta t W^{n+1} \tag{53}$$

where W denotes $\frac{\partial E}{\partial t}$. The resultant solution $[E \quad W]^T$ is then stored as a column vector in $\mathbf{F}_E$, and $\mathbf{F}_E$ is orthogonalized, which is then used to obtain a reduced matrix $\mathbf{M}_{Ar}=\mathbf{F}_E^T\mathbf{M}_A\mathbf{F}_E$. When progressively adding a solution vector into $\mathbf{F}_E$, repeating eigenvalues will be observed from the eigenvalue solution of $\mathbf{M}_{Ar}$. These repeating eigenmodes that satisfy (17), when their weights become dominant in the field solution based on (42), and the difference between repeating eigenvalues identified at adjacent steps that is within an error tolerance ϵ_2 shown in (43), can be multiplied in front by $\mathbf{F}_E$ to obtain a complete set of stable modes $\mathbf{V}_{A,st}$.

D. Dispersion Analysis

In a vacuum or free space, the following dispersion relation holds true:

$$\omega^2=c^2(k_x^2+k_y^2+k_z^2) \tag{54}$$

where ω is angular frequency; c is the speed of light; k_x, k_y, and k_z are wavenumber along x-, y-, and z-directions, respectively.

However, the above relationship does not hold true in an inhomogeneous problem because the solution of Maxwell's equations subject to all the boundary conditions at the material interfaces is not a plane wave. In fact, for a lossless inhomogeneous problem, we can derive the following relationship for dispersion analysis:

$$\omega^2=\xi \tag{55}$$

where ξ is the eigenvalue of the $1/\epsilon\nabla\times(1/\mu\nabla\times)$ operator obtained from the inhomogeneous problem. This relationship can be readily obtained by starting from the second-order vector wave equation in an inhomogeneous problem, and finding its source-free solution in frequency domain. Numerically, this leads to a frequency-domain counterpart of (6) except that $\mathbf{D}_\sigma$ term is not present in lossless cases. Hence, the eigenvalue ξ is the eigenvalue of $\mathbf{M}$ only shown in (7). In a vacuum or free space, the ξ would revert to the right-hand side of the commonly used dispersion relation (54). But for general inhomogeneous problems, it does not. For lossy inhomogeneous problems, from the frequency-domain counterpart of (6) which is the same as (46), we can see the following relationship holds true:

$$j\omega=\lambda \tag{56}$$

where λ is the eigenvalue of the quadratic eigenvalue problem shown in (8).

Now, we can analyze the dispersion error of the proposed method for both single-material and inhomogeneous cases. For lossless problems, we solve the following equation in the proposed explicit time marching:

$$\frac{d^2y_i}{dt^2}+\xi_i y_i=0 \tag{57}$$

as shown in [21], where ξ_i is the ith eigenvalue. To obtain the above, we expand the field solution $E(t)$ by stable eigenmodes found in the preprocessing step as $\mathbf{V}_{E,st}y(t)$, and multiply the numerical system (6) by $\mathbf{V}_{E,st}^T$ on both sides. The leap-frog-based first-order solution given in [21] also naturally leads to (57) by eliminating the magnetic field unknown. Since the central-difference scheme is used in the proposed method, for a time-harmonic input of $e^{j\omega t}$, we obtain the following discretization of (57)

$$-4\sin^2(\omega\Delta t/2)+\Delta t^2\xi_i=0. \tag{58}$$

When $\omega\Delta t$ approaches zero, i.e., the time step is chosen based on good sampling accuracy, it is evident that we will obtain (55). In addition, it can be seen that if ξ_i is large, a very small time step needs to be used to control dispersion error. However, if the modes having large ξ_i are completely removed as done in the proposed method, a large time step can be used without degrading the dispersion accuracy. For inhomogeneous lossy problems, similarly, by discretizing (51) in time, we can see when $\omega\Delta t$ approaches zero, we obtain (56). As for the accuracy of ξ in (55) and λ in (56), they are obtained by central-difference-based space discretization since the FDTD scheme is used. Hence, the accuracy obeys the accuracy of the central difference. For example, in free space, ξ in the proposed method is equal to $c^2(\frac{4\sin^2(k_x\Delta x/2)}{\Delta x^2}+\frac{4\sin^2(k_y\Delta y/2)}{\Delta y^2}+\frac{4\sin^2(k_z\Delta z/2)}{\Delta z^2})$. As a result, it becomes $c^2(k_x^2+k_y^2+k_z^2)$ when the space step is small. Similarly, it also approaches to the exact value in homogeneous problems when space discretization is refined.

IV. Numerical Results

A. Demonstration of Unconditional Stability

First, we demonstrate the unconditional stability of the proposed method by simulating an example that has an analytical solution. The example is a three-dimensional (3-D) parallel-plate structure filled with a lossy dielectric of conductivity 0.3 S/m. The height, width, and length of the structure are 1, 6, and 900 μm, along each of which the space step is 0.2, 1.2, and 100 μm, respectively. A current source is launched from the bottom plate to the top plate at the near end of the parallel plate structure, while voltages are sampled at both the near end and the far end. The current waveform is a Gaussian derivative pulse of $I(t)=2(t-t_0)e^{-(t-t_0)^2/\tau^2}$ with $\tau=0.2$ s and $t_0=4\tau$ s.

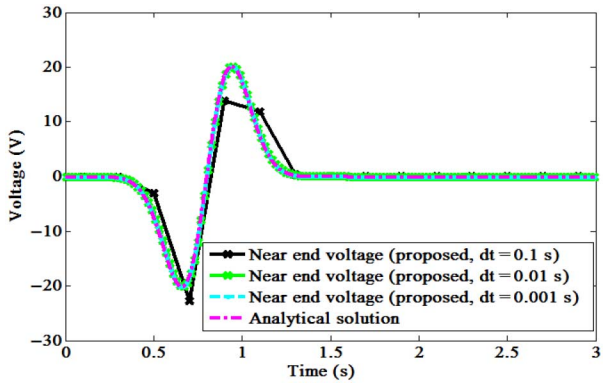

Fig. 1. Simulation of a lossy parallel-plate structure.

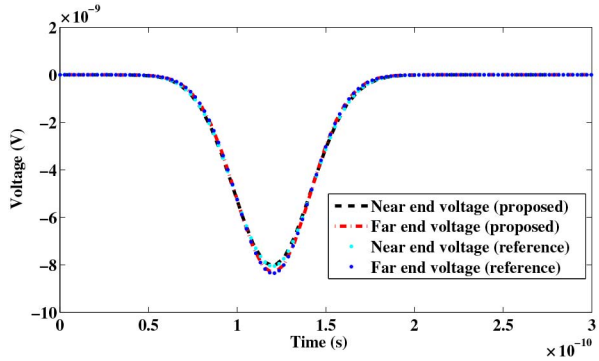

Fig. 2. Simulation of a lossy on-chip interconnect of metal conductivity $\sigma = 5e + 7$ S/m.

Due to the small space step of the structure, the traditional FDTD must use a time step as small as $6.58e - 16$ s to ensure the stability of the time-domain simulation. In contrast, for the same space step, the proposed method can use an arbitrarily large time step without becoming unstable. For example, to use an infinitely large time step, we only need to keep zero-eigenvalue modes while discarding others. In Fig. 1, we plot the results generated with the time step of 0.1, 0.01, and 0.001 s, respectively, in comparison with analytical data. It is evident that the proposed method is stable, while with the same time steps, the conventional FDTD simply diverges. Moreover, when the time step satisfies accuracy requirements for the given input spectrum, such as $\Delta t = 0.01$ s and $\Delta t = 0.001$ s, the results generated by the proposed method are not only stable but also accurate, as can be seen from Fig. 1. Notice that the time step of 0.01 s is 13 orders of magnitude larger than that of the CFL time step, which also verifies the capability of the proposed method in controlling dispersion error. Both the algorithm described in Sections III-A and III-B and the diagonal-preserving algorithm in Section III-C are used to simulate this example. The results are on top of each other.

B. Demonstration of the Efficiency and Accuracy of the Proposed Method

We have simulated a suite of examples to examine the performance of the proposed methods. The algorithm described in Sections III-A and III-B is used to simulate all examples. Some examples are also simulated by the diagonal-preserving algorithm described in Section III-C.

1) Inhomogenous On-Chip Lossy Interconnect: The second example is a 3-D inhomogeneous on-chip interconnect structure with a large metal conductivity of $5e + 7$ S/m and multiple layers of dielectrics. The dimension of the structure is 2000 μm×300 μm×100 μm, along which the mesh size is 200, 50, and 16.67 μm, respectively. The input current source is the same as that in the first example, but with $\tau = 3e - 11$ s. In the preprocessing step, the accuracy-control parameters ϵ_1 and ϵ_2 are chosen as 10^{-4} and 10^{-5}, respectively. The FDTD solutions are sampled every 20 steps, i.e., $p = 20$. Six stable modes are identified from the preprocessing step, whose eigenvalues are -3.044×10^{13}, -1.979×10^{12}, $-3.098 \times 10^{5} \pm 6.317 \times 10^{8} j$, and $-2.92 \times 10^{6} \pm 4.8 \times 10^{11} j$, respectively. In conventional FDTD, the time step, constrained by the smallest space step, must be chosen as small as 5.2577×10^{-14} s for a stable simulation. In contrast, the time step in the proposed method is 2.9412×10^{-12} s solely determined by accuracy. The total CPU time of the proposed method including both the preprocessing step and the explicit marching step is 28.422 s, whereas the total time of the conventional FDTD is 362.588 s. In Fig. 2, we compare the solution obtained from the proposed method with that from the FDTD at the near and far end of the interconnect. Excellent agreement is observed at both ends. Notice that in this example, the near-end and far-end waveforms are different due to a relatively high frequency, and hence a nonstatic effect. We also compare the *entire* solution with the FDTD solution by assessing $||u - u_{ref}||/||u_{ref}||$ across the whole time window, where u denotes the vector of the electric and magnetic field solutions at all points obtained from the proposed method, and u_{ref} is the same but from the conventional FDTD. The average $||u - u_{ref}||/||u_{ref}||$ is shown to be 0.226%, revealing an excellent agreement between the proposed method and the conventional FDTD at all points in space and across the whole time window.

2) Lossy Parallel Plate Structure Excited by a High-Frequency Pulse: In this example, we consider the same 3-D parallel plate structure simulated in Section IV-A but with $\sigma = 0.1$ S/m, and a fast Gaussian derivative pulse having a maximum input frequency of 34 GHz. To simulate this example, a conventional explicit FDTD method requires a time step as small as 6.5805×10^{-16} s to maintain the stability of the time-domain simulation because the smallest space step is 0.1 μm. In contrast, the proposed explicit method is able to use a large time step of 2.9412×10^{-12} s solely determined by accuracy to generate accurate and stable results. In the preprocessing step, the FDTD solutions are sampled every 40 steps, i.e., $p = 40$. The accuracy-control parameters ϵ_1 and ϵ_2 are chosen as 10^{-4} and 10^{-5}, respectively. Two stable eigenmodes are identified, whose eigenvalues are -1.0993×10^{8} and -1.1184×10^{10}, respectively. In Fig. 3, the voltage waveforms simulated by the proposed method are shown to agree very well with those generated by the conventional explicit FDTD. The total CPU time required by the proposed method is 113.50898 s including both the preprocessing step and the explicit marching

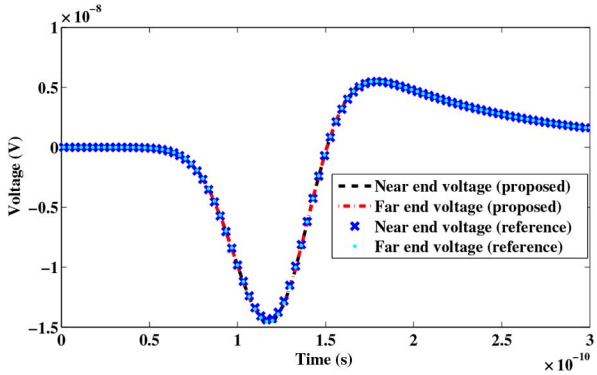

Fig. 3. Simulation of a lossy parallel plate waveguide of $\sigma = 0.1$ S/m.

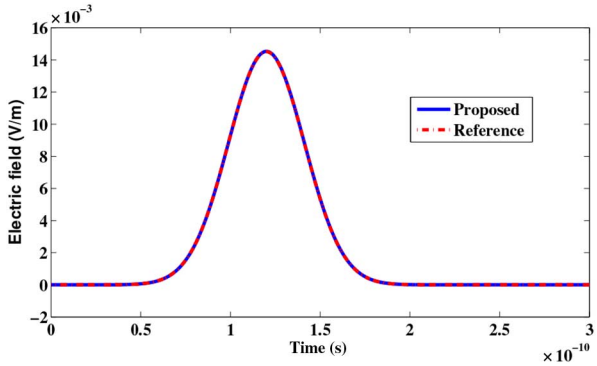

Fig. 4. Simulation of an antenna with a lossy dielectric cylinder.

step, whereas the CPU time of the conventional FDTD is 19 079.793260 s, yielding a speedup of approximately 170. The diagonal-preserving formulation described in Section III-C was also used to simulate this example, the speedup of which is shown to be about 186.

3) Radiation of a Dipole Antenna in the Presence of Lossy Dielectrics: Next example is the radiation of a dipole antenna in the presence of a lossy dielectric cylinder of conductivity 0.1 S/m, the computational domain of which is truncated by a PML. The dipole of length 75 μm is placed at the center of a solution domain of dimension 900 μm×300 μm×100 μm. The PML region has 20 grid cells all around the solution domain with a uniform cell size of 81.8, 33.33, and 25 μm in x-, y-, and z-directions, respectively. The lossy rectangular cylinder has a length of 81.8 μm, width 33.33 μm, and height 75 μm. The smallest mesh size is approximately 1.6364 μm. The source is the same as that in the second example. The solutions are sampled every nine steps in the preprocessing. The ϵ_1 and ϵ_2 are chosen as 10^{-3} and 10^{-5}, respectively. The conventional FDTD uses a time step of 5.44×10^{-15} s and takes 12 592.07 s to complete the whole simulation, whereas the proposed method uses a time step of 6.4805×10^{-14} s and takes 1053.05 s to complete the simulation. There are 32 stable eigenmodes identified from the proposed method, whose eigenvalues are $-7.23 \times 10^5 \pm 2.31990 \times 10^{12}$, $-2.8007 \times 10^7 \pm 4.1638 \times 10^{12} j$, $-3.0126 \times 10^5 \pm 5.2944 \times 10^{12} j$, $-6.8298 \times 10^7 \pm 6.782805 \times 10^{12} j$, $-2.16576 \times 10^6 \pm 7.522289 \times 10^{12} j$, and others. The speedup of the proposed method is approximately 12, without sacrificing accuracy as can be seen from Fig. 4.

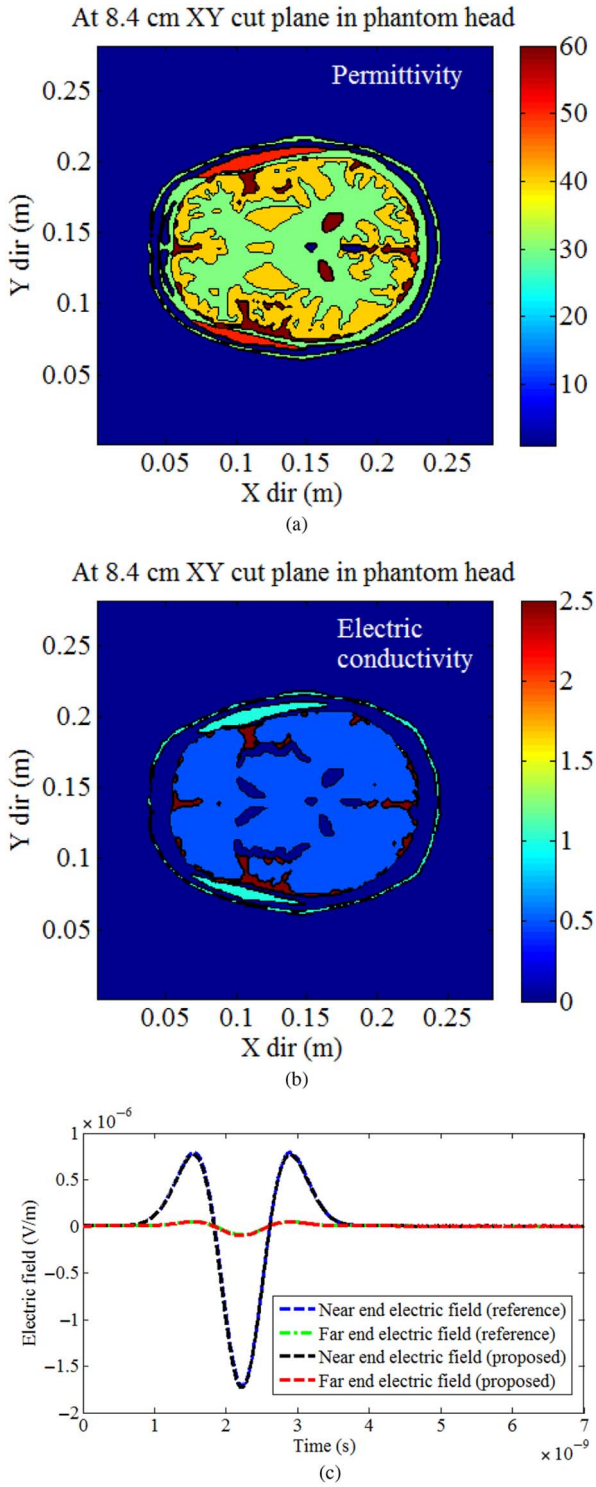

Fig. 5. Simulation of a phantom head beside a wire antenna. (a) Relative permittivity distribution in a cross section of the phantom head at a height of 8.4 cm (XY-cut). (b) Electric conductivity distribution in a cross section of the phantom head at a height of 8.4 cm (XY-cut). (c) Simulated electric field at two points of the phantom head in comparison with reference FDTD solutions.

4) Phantom Head Beside a Wire Antenna: In previous examples, the structures simulated involve fine features relative to working wavelength. This is understood because only in

TABLE I
CPU TIME AND MEMORY COMPARISON

Example	N	CPU time (s) (conventional)	CPU time (s) (proposed)	Memory (conventional)	Memory (proposed)
On-chip interconnect	1 729	362.59	28.42	152.74 kB	659.62 kB
Lossy parallel plate	933	19 079.79	113.51	79.24 kB	191.29 kB
Dipole antenna	1 863	12 592.07	1 053.05	33.13 MB	33.53 MB
Phantom head	49 160 302	2.03e+6	90 106	6.23 GB	9.17 GB

these structures, there is a need to enlarge the time step, since the time step required by the CFL stability condition is smaller than that required by accuracy. In the last example, to examine the performance of the proposed method in a comprehensive fashion, we simulate an example in two settings: without fine features relative to working wavelength and with fine features. This example is also much larger than previous examples in both unknown number and electrical size.

The example is a large-scale phantom head example [18] beside a wire antenna, having more than 48 million unknowns. The dimension of the phantom head is 28.16 cm×28.16 cm×17.92 cm. The relative permittivity and conductivity distributions of the phantom head are shown in Fig. 5(a) and (b), respectively, at the height of 8.4 cm. The number of discretization cells in the solution domain is 255×255×127, while the number of cells used in PML is 30 along each direction. The total number of cells is thus 315×315×187. The smallest space step along x-, y-, and z-directions is, respectively, 1.1, 1.1, and 1.4 mm. The input current source has a waveform of Gaussian derivative, located at $x = 14.52$ cm and $y = 26.18$ cm. In the first simulation, we do not consider fine tissues in this example, and let the space step solely determined by accuracy. As a result, the time step required by stability and that by accuracy are at the same level. Thus, both traditional FDTD and the proposed method employ the same time step of $2.2680e-12$ s. In the preprocessing step, 74 stable eigenmodes are identified with a choice of $\epsilon_1 = 10^{-5}$ and $\epsilon_2 = 10^{-7}$. The smallest eight nonzero eigenvalues are, respectively, $-8.5423e6 \pm 15474e10j$, $-1.489e7 \pm 5.414e10j$, $-3.612e7 \pm 1.2275e11j$, and $-1.859e7 \pm 1.708e11j$. The total CPU time cost by the traditional FDTD is 68 881.738268 s, whereas the total CPU time of the proposed method including both preprocessing and explicit time-marching is only 38 343.45917 s. Thus, the speedup of the proposed method is 1.7937, although the structure does not involve fine features and the same time step is used in the proposed method. The theoretical reason for this speedup is the same as that analyzed in [21] for lossless cases. The electric field waveforms simulated from the proposed method at point (14.52, 27.72, 10.92) cm and point (14.52, 0.22, 10.92) cm are compared with that of the conventional FDTD in Fig. 5(c). Excellent agreement is observed.

Next, we consider the small tissues involved in the human head, for which the smallest space step is reduced to 0.044 mm. As a result, the conventional FDTD has to reduce the time step accordingly to $1.4672e-13$ s, whereas the proposed method is able to use the same time step as before. It takes the proposed method 90 106 s to finish the entire simulation, whereas the conventional FDTD cannot finish the simulation in 10 days even though we enlarge the cell size in the regions without fine tissues by two times. Based on the CPU time cost of the FDTD at each time step, the projected run time of FDTD is $2.0330e+06$ s; thus, the speedup of the proposed method over the conventional FDTD is greater than 23 in this example.

In Table 1, we summarize the CPU time and memory used by the proposed method in comparison with the conventional FDTD for each example, where N denotes the total number of electric field and magnetic field unknowns. The additional memory used in the proposed method is mainly the storage of $\mathbf{F}_e$ matrix, whose size is N_e by k'. Notice that the $\mathbf{V}_{E,st}$ in (44) is stored in $\mathbf{F}_e$ and $\mathbf{V}_{r,st}$ (a small matrix of size $k' \times k$), instead of being separately stored as a new matrix. The expression of (44) is used for computation instead of forming $\mathbf{V}_{E,st}$ explicitly. For example, the $\tilde{\mathbf{V}}_{E,st}$ in (35) and (36) is nothing but $\mathbf{F}_e$ multiplied by orthogonalized $\mathbf{V}_{r,st}$. Furthermore, it is worth mentioning that the reduced eigenvalue problem formulated in this work is of a small size $O(k')$, and hence its storage is negligible as compared to the storage of $\mathbf{F}_e$.

5) Comparisons With Implicit Unconditionally Stable FDTD Methods: In this section, we compare the accuracy, stability, and efficiency of the proposed explicit method with those of two implicit FDTD methods. One is the ADI-FDTD method [3], [4], the other is a recently developed one-step implicit unconditionally stable FDTD method [24]. This new implicit method is very convenient for implementation since only one time instant needs to be changed in the conventional FDTD method to make the FDTD unconditionally stable. The unconditional stability of this new method is also theoretically proved in [24].

The example considered is a free-space wave propagation problem, the analytical solution of which is known. Hence, we can use this example to accurately assess the performance of the three unconditionally stable methods. The computational domain has a length (L) of 9 mm and a width (W) of 9 mm. The incident field is a $\hat{y}$-polarized electric field propagating along x-direction, whose expression is $\mathbf{E} = \hat{y} f(t - x/c)$, where the pulse $f(t) = exp(-(t - t_0)^2/\tau^2)$, with $\tau = (1/3) \times 10^{-10}$ s, and $t_0 = 4\tau$ s. Since the computational domain is filled by air, the boundary condition on the four outermost boundaries is analytically known, which is the tangential incident field since the scattered field is zero. Hence, we impose such an analytical absorbing boundary condition on $x = 0$, L, and $y = 0$, W, respectively. The computational domain is discretized into 50 cells along both x- and y-directions, which is determined based on the input spectrum. The 26th cell size along x and y directions is 20 times smaller than the rest of the cell size that is $L/50$, and hence being $L/1000$. As a result, the time step required by CFL stability condition is 20 times smaller than the

time step required by accuracy. We define the following time step:

$$\Delta t = \frac{CFLN}{c\sqrt{1/\min(dx)^2 + 1/\min(dy)^2}} \tag{59}$$

where CFLN is clearly the ratio between the time step used in simulation to the time step required by the CFL condition. Based on the time step required by accuracy, the CFLN can be as large as 20. The observation point is chosen at the center of the computational domain, specifically, point $(x = 4.32, y = 4.41)$ mm, to examine the dispersion error, as well as entire solution accuracy of the three unconditionally stable methods.

In Fig. 6(a), we plot the E_y fields obtained from the ADI method at the observation point, with CFLN $= 2$ and 4, respectively. If we enlarge CFLN to be 5 or larger, the ADI scheme is found to be unstable in this example, which may be attributed to the relatively rapid change in the space step in the computational domain, as the scheme is found to be stable if the discretization is made uniform. When the ADI is stable, as can be seen from Fig. 6(a), the ADI results agree well with the reference solution which is the analytical solution in this example. In Fig. 6(b), we plot the E_y field obtained from the proposed method at the same observation point. Obviously, the proposed method is stable, and also accurate not only for CFLN $= 4$ but also for large CFLN such as 10, 15, and 20. In Fig. 6(c), we plot the fields obtained from the one-step implicit method [24] with CFLN ranging from 4 to 20. The results are also shown to be stable and accurate. However, compared to the proposed method, the accuracy is lower.

In addition to comparing the time-domain waveforms, we have also quantitatively examined the dispersion error of the three methods. The time-domain field at the observation point and the incident field at the left boundary are Fourier transformed, and the phase difference is extracted between the two Fourier transforms, from which we find the average phase velocity in a range of frequencies from 3 to 15 GHz as a function of CFLN. In Fig. 7, we plot the ratio of the numerical phase velocity (V_p) to the ideal phase velocity for proposed method in comparison with the ADI and the one-step implicit unconditionally stable method. The dispersion error of the proposed method is shown to be much less than that of the other two methods, with phase velocity ratio in the range of 0.9924 and 0.9969. As far as the theoretical reason is concerned, in the proposed explicit unconditionally stable time marching, only stable eigenmodes are kept in the numerical system, and these stable eigenmodes have an eigenvalue ξ that can be accurately sampled by the given time step, and hence ensuring accuracy. In contrast, in implicit unconditionally stable methods, the unstable eigenmodes for the given time step that have large ξ are not removed. Instead, they are kept in the numerical system, and present at each time instant. When a large time step is used, although the unstable modes are suppressed to be stable by an implicit time integration scheme, they cannot be accurately simulated by the given time step based on sampling accuracy, and hence deteriorating the overall accuracy of the field solution. As can be observed from Fig. 7, the dispersion error of the implicit

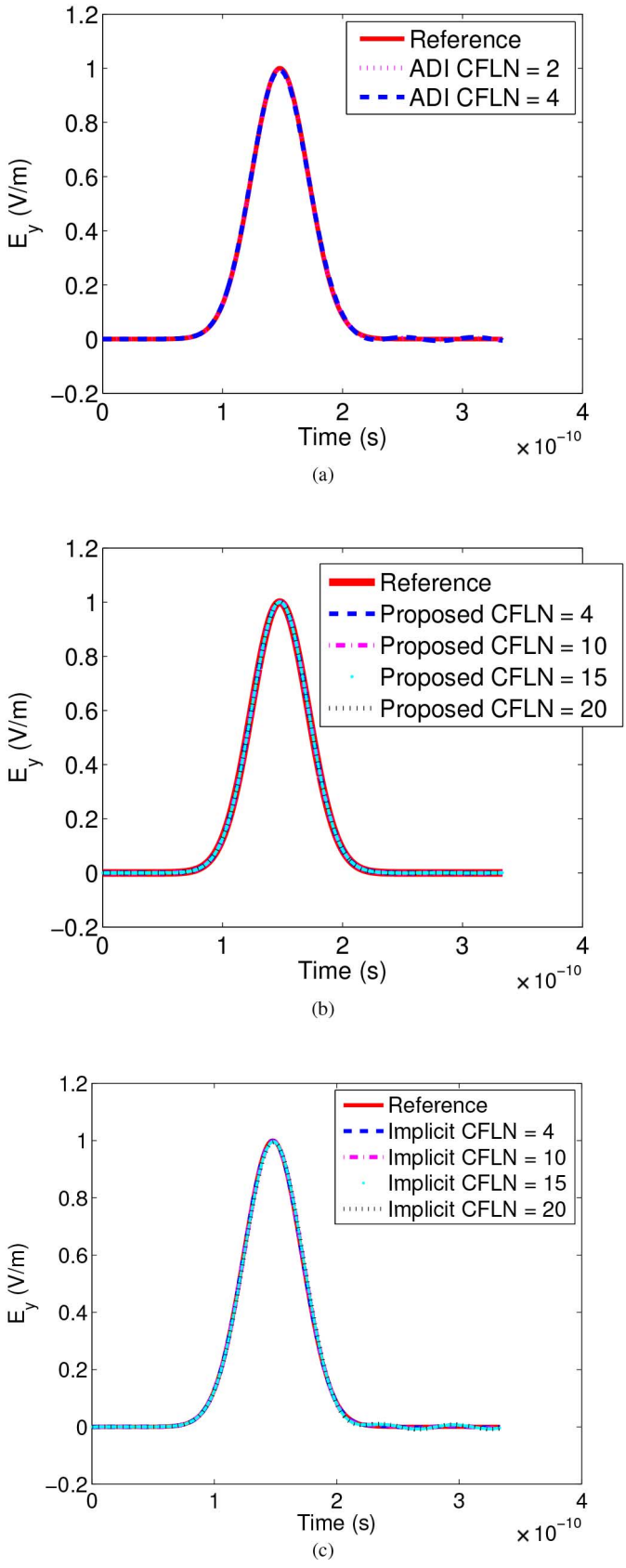

Fig. 6. Simulated fields as a function of CFLN. (a) ADI-FDTD. (b) Proposed method. (c) One-step implicit unconditionally stable FDTD [24].

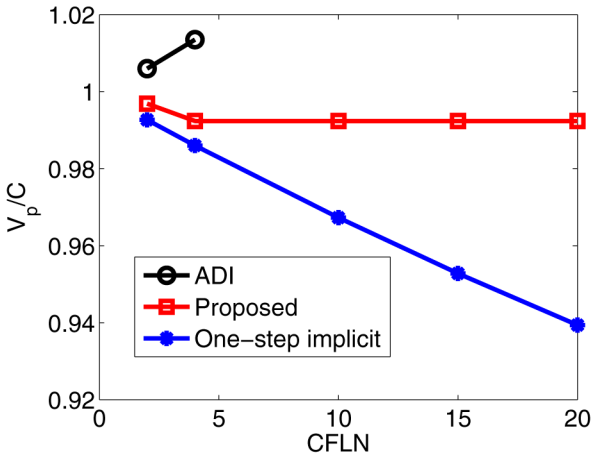

Fig. 7. Comparison of dispersion error characterized by phase velocity ratio among three methods.

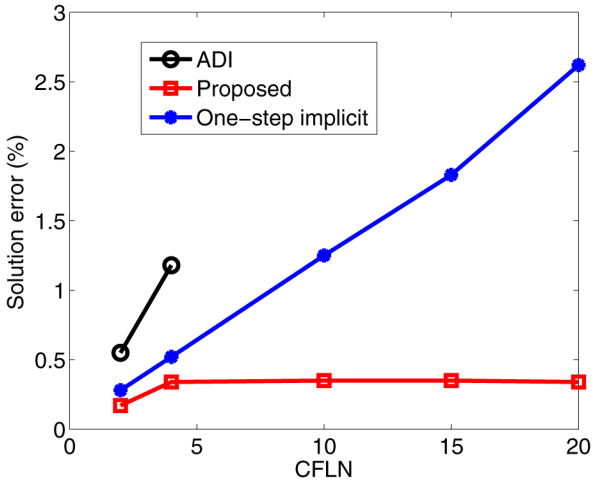

Fig. 8. Comparison of solution error among three methods.

methods increases when CFLN increases, whereas the proposed method has a well-controlled dispersion error.

Dispersion error is only one aspect of the time-domain solution error. To assess the entire error, in Fig. 8, we plot the solution error measured by $||E(t) - E_{ref}(t)||/||E_{ref}(t)||$ as a function of CFLN for three different methods, where $E_{ref}(t)$ is the analytical solution at the observation point at all time. Less than 0.35% error is observed in the proposed method, whereas the two implicit methods are shown to have a larger error, which also increases with CFLN.

In addition to stability and accuracy, we have also compared the computational efficiency of the proposed method with the implicit unconditionally stable methods. For the phantom head example having over 48 million unknowns, the one-step implicit method [24] with a GMRES-based iterative matrix solver takes 86 656.4 s to finish the entire simulation, whereas the proposed method only costs 38 343.4 s. Therefore, preserving the matrix-free property of the original FDTD is another important advantage one can benefit from the proposed explicit and unconditionally stable method. For the phantom head example having fine tissues simulated in Section IV-B4, the implicit method [24] is found to be unstable at the late time.

V. Conclusion

In this paper, we have theoretically analyzed the root cause of the instability of an explicit FDTD method for the analysis of general 3-D lossy problems, where the materials are inhomogeneous, and both dielectrics and conductors can be lossy. Based on this root cause analysis, we develop an explicit FDTD that is unconditionally stable for analyzing general 3-D lossy electromagnetic problems. In this method, we fix the instability from the root by completely eliminating the source of instability; and we retain the strength of an explicit FDTD in avoiding matrix solutions. The dispersion error of the proposed method is also theoretically analyzed for general inhomogeneous settings and numerically examined. Numerical experiments and comparisons with implicit unconditionally stable methods, as well as the conventional FDTD, have demonstrated the unconditional stability, accuracy, and efficiency of the proposed method. The essential idea of the proposed method for handling general lossy problems is also applicable to other time-domain methods.

References

[1] K. S. Yee, "Numerical solution of initial boundary value problems involving Maxwell's equations in isotropic media," *IEEE Trans. Antennas Propag.*, vol. 14, no. 5, pp. 302–307, May 1966.

[2] A. Taflove and S. C. Hagness, *Computational Electrodynamics: The Finite-Difference Time-Domain Method*. Norwood, MA, USA: Artech House, 2000.

[3] T. Namiki, "A new FDTD algorithm based on alternating-direction implicit method," *IEEE Trans. Microw. Theory Tech.*, vol. 47, no. 10, pp. 2003–2007, Oct. 1999.

[4] F. Zheng, Z. Chen, and J. Zhang, "A finite-difference time-domain method without the Courant stability conditions," *IEEE Microw. Guided Wave Lett.*, vol. 9, no. 11, pp. 441–443, Nov. 1999.

[5] G. Sun and C. W. Trueman, "Unconditionally stable Crank–Nicolson scheme for solving two-dimensional Maxwell's equations," *Electron. Lett.*, vol. 39, no. 7, pp. 595–597, Apr. 2003.

[6] J. Lee and B. Fornberg, "A splitting step approach for the 3-D Maxwell's equations," *J. Comput. Appl. Math.*, vol. 158, pp. 485–505, 2003.

[7] G. Zhao and Q. H. Liu, "The unconditionally stable pseudospectral time-domain (PSTD) method," *IEEE Microw. Wireless Compon. Lett.*, vol. 13, no. 11, pp. 475–477, Nov. 2003.

[8] J. Shibayama, M. Muraki, J. Yamauchi, and H. Nakano, "Efficient implicit FDTD algorithm based on locally one dimentional scheme," *Electron. Lett.*, vol. 41, no. 19, pp 1046–1047, Sep. 2005.

[9] V. E. do Nascimento, B.-H. V. Borges, and F. L. Texeira, "Split-field PML implimentation for the unconditionally stable LOD-FDTD method," *IEEE Microw. Wireless Compon. Lett.*, vol. 16, no. 7, pp. 398–400, Jul. 2006.

[10] Y. S. Chung, T. K. Sarkar, B. H. Jung, and M. Salazar-Palma, "An unconditionally stable scheme for the finite-difference time-domain method," *IEEE Trans. Microw. Thoery Tech.*, vol. 59, no. 1, pp. 56–64, Jan. 2011.

[11] Z. Chen, Y. T. Duan, Y. R. Zhang, and Y. Yi, "A new efficient algorithm for the unconditionally stable 2-D WLP-FDTD method," *IEEE Trans. Antennas Propag.*, vol. 61, no. 7, pp. 3712–3720, Jul. 2013.

[12] Y. Yu and Z. Chen, "Towards the development of an unconditionally stable time-domain meshless method," *IEEE Trans. Microw. Theory Tech.*, vol. 58, no. 3, pp. 578–586, Mar. 2010.

[13] Z.-Y. Huang, L.-H. Shi, B. Chen, and Y. H. Zhou, "A new unconditionally stable scheme for FDTD method using associated Hermite orthogonal functions", *IEEE Trans. Antennas Propag.*, vol. 62, no. 9, pp. 4804–4808, Sep. 2014.

[14] E. L. Tan, "Fundamental schemes for efficient unconditionally stable implicit finite-difference time-domain methods," *IEEE Trans. Antennas Propag.*, vol. 56, no. 1, pp. 170–177, Jan. 2008.

[15] A. Ecer, N. Gopalaswamy, H. U. Akay, and Y. P. Chien, "Digital filtering techniques for parallel computation of explicit schemes," *Int. J. Comput. Fluid Dyn.*, vol. 13, no. 3, pp. 211–222, 2000.

[16] C. Chang and D. S. Costas, "A spatially filtered finite-difference time-domain scheme with controllable stability beyond the CFL limit," *IEEE Trans. Microw. Theory Tech.*, vol. 61, no. 1, pp. 351–359, Mar. 2013.
[17] F. Tisseur and K. Meerbergen, "The quadratic eigenvalue problem," *SIAM Rev.*, vol. 43, no. 2, pp. 235–286, 2001.
[18] G. Zubal, C. R. Harrell, E. O. Smith, Z. Rattner, G. Gindi, and P. B. Hoffer, "Computerized three-dimensional segmented human anatomy," *Med. Phys.*, vol. 21, no. 2, pp. 299–302, 1994.
[19] Q. He, H. Gan, and D. Jiao, "Explicit time-domain finite-element method stabilized for an arbitrarily large time step," *IEEE Trans. Antennas Propag.*, vol. 60, no. 11, pp. 5240–5250, Nov. 2012.
[20] M. Gaffar and D. Jiao, "An explicit and unconditionally stable FDTD method for 3-D electromagnetic analysis," in *Proc. IEEE Int. Microw. Symp. (IMS)*, Jun. 2013, 4 pp.
[21] M. Gaffar and D. Jiao, "An explicit and unconditionally stable FDTD method for electromagnetic analysis," *IEEE Trans. Microw. Theory Tech.*, vol. 62, no. 11, pp. 2538–2550, Nov. 2014.
[22] M. Gaffar and D. Jiao, "An explicit and unconditionally stable FDTD method for the analysis of general 3-D lossy problems," in *Proc. IEEE Int. Microw. Symp. (IMS)*, Jun. 2014, 4 pp.
[23] M. Gaffar and D. Jiao, "Diagonal-preserving explicit and unconditionally stable FDTD method for analyzing general lossy electromagnetic problems," in *Proc. IEEE Antennas Propag. Soc. Int. Symp.*, Jul. 2014, pp. 165–166.
[24] M. Gaffar and D. Jiao, "A simple implicit and unconditionally stable FDTD method by changing only one time instant," in *Proc. IEEE Antennas Propag. Soc. Int. Symp.*, Jul. 2014, pp. 725–726.

Md Gaffar received the B.Sc. degree in electrical engineering from the Bangladesh University of Engineering and Technology (BUET), Dhaka, Bangladesh, in 2009. Since 2011, he has been pursuing the Ph.D. degree in electrical engineering at the School of Electrical and Computer Engineering, Purdue University, West Lafayette, IN USA.

His research interests include computational electromagnetics and semiconductor physics.

Mr. Gaffar was the recipient of academic awards in recognition of his research achievements, including the Best Poster Award (among all groups) and Best Project Award in Communication and Electromagnetic in EEE Undergraduate Project Workshop (EUProW) 2009. At Purdue, his research has been recognized by the IEEE International Microwave Symposium Best Student Paper Finalist Award in 2013 and 2015, and the 2014 IEEE International Symposium on Antennas and Propagation Honorable Mention Paper Award.

Dan Jiao (S'00–M'02–SM'06) received the Ph.D. degree in electrical engineering from the University of Illinois at Urbana-Champaign, Champaign, IL, USA, in 2001.

She then worked with the Technology Computer-Aided Design (CAD) Division, Intel Corporation, Santa Clara, CA, USA, until September 2005, as a Senior CAD Engineer, Staff Engineer, and Senior Staff Engineer. In September 2005, she joined Purdue University, West Lafayette, IN, USA, as an Assistant Professor with the School of Electrical and Computer Engineering, where she is currently a Professor. She has authored 3 book chapters and over 200 papers in refereed journals and international conferences. Her research interests include computational electromagnetics, high-frequency digital, analog, mixed-signal, and RF integrated circuit (IC) design and analysis, high-performance VLSI CAD, modeling of microscale and nanoscale circuits, applied electromagnetics, fast and high-capacity numerical methods, fast time-domain analysis, scattering and antenna analysis, RF, microwave, and millimeter-wave circuits, wireless communication, and bio-electromagnetics.

Dr. Jiao has served as a Reviewer for many IEEE journals and conferences. She is an Associate Editor of the IEEE TRANSACTIONS ON COMPONENTS, PACKAGING, AND MANUFACTURING TECHNOLOGY. She was among the 85 engineers selected throughout the nation for the National Academy of Engineering's 2011 U.S. Frontiers of Engineering Symposium. She has been named a University Faculty Scholar by Purdue University since 2013. She was the recipient of the 2013 S. A. Schelkunoff Prize Paper Award of the IEEE Antennas and Propagation Society, which recognizes the Best Paper published in the IEEE TRANSACTIONS ON ANTENNAS AND PROPAGATION during the previous year, the 2010 Ruth and Joel Spira Outstanding Teaching Award, the 2008 National Science Foundation (NSF) CAREER Award, the 2006 Jack and Cathie Kozik Faculty Start up Award (which recognizes an outstanding new faculty member of the School of Electrical and Computer Engineering, Purdue University), a 2006 Office of Naval Research (ONR) Award under the Young Investigator Program, the 2004 Best Paper Award presented at the Intel Corporations annual corporate-wide technology conference (Design and Test Technology Conference) for her work on generic broadband model of high-speed circuits, the 2003 Intel Corporations Logic Technology Development (LTD) Divisional Achievement Award, the Intel Corporations Technology CAD Divisional Achievement Award, the 2002 Intel Corporations Components Research the Intel Hero Award (Intel-wide she was the tenth recipient), the Intel Corporations LTD Team Quality Award, and the 2000 Raj Mittra Outstanding Research Award presented by the University of Illinois at Urbana-Champaign.